Caucasian Journal of Science
ISSN: 2148-6840
https://doi.org/10.48138/cjo.1795498
Year: 2025
Volume:12 Issue: 2
To Cite: Keşkek Karabulut, Y. (2025). Investigation of Biopesticide Properties of Garlic Extract Compounds Suitable for Sustainable Agriculture and Food Safety against White Mold Disease in Sunflower Production. Caucasian Journal of Science, 12(2), 100-122

Ayçiçeği Üretiminde Beyaz Küf Hastalığına Karşı Sarımsak Özütü Bileşiklerinin Sürdürülebilir Tarım ve Gıda Güvenliğine Uygun Biyopestisit Özelliklerinin Araştırılması

Investigation of Biopesticide Properties of Garlic Extract Compounds Suitable for Sustainable Agriculture and Food Safety against White Mold Disease in Sunflower Production

Yasemin KEŞKEK KARABULUT[1]

Kimya/ Chemistry **Araştırma Makalesi / Research Article**

Makale Bilgileri

Geliş Tarihi
02.10.2025
Kabul Tarihi
19.12.2025
Anahtar Kelimeler
Sarımsak Özütü
Sclerotinia sclerotiorum
Moleküler Doking
Biyopestisit
Sürdürülebilir Tarım

Öz

Bu çalışmada, ayçiçeği üretiminde ciddi verim kayıplarına yol açan Beyaz Küf Hastalığı (Sclerotinia sclerotiorum)'na karşı, çevre dostu ve sürdürülebilir bir biyolojik mücadele yöntemi geliştirilmesi amaçlanmıştır. Kimyasal pestisitlerin olumsuz etkilerini azaltmak ve gıda güvenliğine katkı sağlamak amacıyla sarımsak özütü bileşiklerinin (Allisin, Allin, Ajoene, Sülfür bileşikleri, Kuersetin, Kaemferol ve Apigenin) biyopestisit potansiyelleri in silico olarak değerlendirilmiştir. Proje kapsamında, moleküler modelleme ve AutoDock Vina yazılımı ile docking çalışmaları gerçekleştirilmiş; bu bileşiklerin patojen proteinlerine bağlanma afiniteleri ve etkileşimleri analiz edilmiştir. Kuersetin (-6.3 kcal/mol), Kaemferol (-6.1 kcal/mol) ve Apigenin (-6.0 kcal/mol) en yüksek bağlanma enerjisi ile öne çıkan bileşikler olmuştur. Bu sonuçlar, özellikle flavonoid grubu bileşiklerin biyopestisit olarak kullanıma uygun olabileceğini göstermektedir. Çalışma sonucunda, flavonoid yapıdaki bileşiklerin patojeni inhibe etme potansiyeli daha yüksek bulunmuş; ayrıca yapısal analizlerde benzen halkası ve hidroksil gruplarının bu etkiyi güçlendirdiği gözlemlenmiştir. Proje, sürdürülebilir tarım uygulamalarına katkı sağlayabilecek doğal pestisitlerin geliştirilmesine yönelik önemli bilimsel veriler sunmuştur.

Article Info

Received
02.10.2025
Accepted
19.12.2025
Keywords
Garlic Extract
Sclerotinia sclerotiorum
Molecular Docking
Biopesticide
Sustainable Agriculture

Abstract

This study aimed to develop an environmentally friendly and sustainable biocontrol approach against White Mold Disease (Sclerotinia sclerotiorum), which causes significant yield losses in sunflower cultivation. In order to reduce the negative impacts of chemical pesticides and contribute to food security, the biopesticide potential of garlic extract compounds (including Allicin, Alliin, Ajoene, sulfur-containing compounds, Quercetin, Kaempferol, and Apigenin) was evaluated in silico using molecular docking techniques. The molecular interactions between these compounds and the pathogen's lectin protein (2X2T structure) were analyzed via AutoDock Vina, and binding affinities were calculated. Among the tested compounds, Quercetin (-6.3 kcal/mol), Kaempferol (-6.1 kcal/mol), and Apigenin (-6.0 kcal/mol) exhibited the most favorable binding energies, suggesting a higher potential as biopesticide agents. These results highlight the promising inhibitory activity of flavonoid compounds compared to sulfur-based constituents. Structural analysis revealed that the presence of benzene rings and hydroxyl (-OH) groups positively influenced the binding and inhibitory effects, while excessive sulfur content reduced efficacy. The findings contribute to the rational design of novel, eco-friendly and sustainable biopesticides, offering valuable insights into functional group effects for future pesticide development in line with Green Deal objectives and sustainable agriculture strategies.

[1] Kırklareli Üniversitesi, Rektörlük, Proje Geliştirme ve Koordinasyon Ofisi- Kırklareli/ Türkiye; e-mail: ykeskekkarabulut@klu.edu.tr; ORCİD:0000-0002-6742-783X (Sorumlu Yazar)

1. INTRODUCTİON

In recent years, the increasing world population has influenced the availability and accessibility of food, making it essential to enhance production efficiency. Among food products, vegetable oils are a significant source of energy, with sunflower oil ranking first as the primary raw material source (Tan & Kaya, 2019). Sunflower is one of the most widely cultivated and produced oilseed crops in Türkiye, meeting nearly half of the country's vegetable oil demand (Semerci, 2019).

According to the 2022 report of the Turkish Statistical Institute (TÜİK), sunflower production reached 2 million tons, with Tekirdağ, Edirne, Adana, and Kırklareli in Türkiye being the leading provinces in production. This indicates that approximately 50% of the national sunflower production demand is supplied by these provinces (Figure 1) (Institute for Agricultural Economics and Policy Development, 2022).

Figure 1. Provinces with the largest share in sunflower production in Türkiye

The suitable climatic conditions for sunflower cultivation are primarily found in the Thrace and Marmara regions, as well as in the transitional zones of Anatolia, the Çarşamba Plain, the Aegean, the Mediterranean, and the cotton-growing areas of Southeastern Anatolia. In addition, sunflower is also cultivated as a confectionary crop in many regions of Türkiye. Regardless of whether for oilseed or confectionary purposes, sunflower is considered a summer row crop.

The vegetable oil obtained from sunflower is rich in the unsaturated fatty acids oleic and linoleic, making its nutritional value and composition comparable to those of olive oil and peanut oil. After oil extraction, the remaining sunflower meal serves as a valuable livestock feed. Containing approximately 44% protein, sunflower meal is superior to meals obtained

from other oilseed crops and is free of toxic substances. Moreover, as sunflowers possess abundant yellow blossoms that attract bees, the plant also holds significant value for beekeepers (Süzer & Çulhacı, 2017).

In the provinces where sunflower cultivation is most intensive, the most common disease observed in sunflowers is Sclerotinia, also known as white mold. This fungal disease is caused by *Sclerotinia sclerotiorum*. It typically emerges during the flowering stage of the plant, leading to lesions, rotting, and wilting on stems, stalks, and leaves. Sclerotinia spreads particularly under humid and cool climatic conditions and can cause severe damage. By decaying plant tissues, the disease results in significant yield losses and considerable economic damage. The control of *Sclerotinia sclerotiorum* is generally carried out through integrated chemical management methods (Koçak & Boyraz, 2021).

Sclerotinia sclerotiorum (Lib.) is a highly destructive pathogen of many economically important crops, including legumes (soybean, pea, and bean) and oilseeds (canola and sunflower). This necrotrophic pathogen exhibits very limited host specificity and has a wide host range encompassing more than 400 plant species, primarily dicotyledonous plants (Hegedus & Rimmer, 2005). Sunflower production is also affected by this pathogen during cultivation, resulting in the occurrence of white mold disease.

Diseases caused by *Sclerotinia sclerotiorum* are among the major factors limiting the production of sunflower (*Helianthus annuus* L.) worldwide (Gulya et al., 2019). *S. sclerotiorum* is also known to cause white mold disease in several other crops, including soybean (*Glycine max* L.), canola (*Brassica napus* L.), and various broadleaf weeds. The fungus produces sclerotia, which possess two germination mechanisms—carpogenic and myceliogenic—allowing it to act as both an airborne and soilborne pathogen. In sunflower, *S. sclerotiorum* is responsible for three distinct diseases: (1) Sclerotinia root rot, basal stem rot, and wilt; (2) Sclerotinia stalk rot; and (3) Sclerotinia head rot and mid-stem rot. The impact of *S. sclerotiorum* on sunflower yield depends on the crop's growth stage at the time of infection, agricultural practices, and environmental conditions (Markell et al., 2015).

Apothecia produced by *Sclerotinia sclerotiorum* can be observed in sunflower fields until the crop canopy closes, and ascospores released from these apothecia may originate from the sunflower field itself. Additionally, ascospores can disperse from adjacent areas where apothecia may be present. These spores settle on the leaves and stems of sunflower plants. In the presence of free moisture and available nutrients, ascospores germinate, infect the

leaves and petioles, and progress toward the stem, causing Sclerotinia stem rot (Harveson, 2011).

Sclerotinia sclerotiorum is a fungal pathogen, commonly known worldwide as "White Mold" due to the characteristic fluffy white mycelial growth observed on the stems of infected plants. Before developing its distinctive cottony mycelium, the pathogen exhibits symptoms on leaves by forming water-soaked lesions that progress downward toward the stem, eventually converting the tissue into necrotic areas (Bolton et al., 2006). Sclerotinia is a polyphagous, necrotrophic, homothallic pathogen that is widespread globally, particularly in temperate regions. It is a destructive plant pathogen capable of infecting over 75 plant families, 278 genera, 408 species, and 42 subspecies. Its most pronounced impact is observed in dicotyledonous crops such as pea, soybean, sunflower, and canola, although it can occasionally affect monocots and grasses as well (Gyanwali et al., 2023).

Figure 2. White mold disease

In recent years, there has been an increase in the use of pesticides to control fungal diseases, such as *Sclerotinia sclerotiorum*, which significantly affect crop yields. Moreover, reducing the risks associated with pesticide pollution has become a key objective in agricultural policy worldwide (Möhring et al., 2020). Accordingly, the European Union aims to reduce both the use and the risk of pesticides by 50% by 2030 (Schebesta & Candel, 2020).

Considering the impacts of global climate change and intensive pesticide usage on species biology and ecological systems, there has been a growing tendency in recent years to adopt alternative control strategies instead of chemical interventions in agricultural fields. This trend has been incorporated into studies related to the European Green Deal and similar initiatives in Türkiye, with targets set to reduce pesticide use or promote the application of natural products by 2030–2050. The European Green Deal seeks to initiate and sustain a comprehensive transformation, prioritizing objectives such as preventing environmental

pollution, conserving biodiversity, and promoting organic farming (Ecer et al., 2021). In alignment with these European goals, Türkiye has developed an action plan under the Green Deal framework (Presidency of Strategy and Budget, 2023). This plan includes a "Sustainable Agriculture" component. Within this context, and based on the EU's objectives for reducing pesticide and antimicrobial use, efforts are planned to minimize the application of these chemicals and to expand the use of alternative control methods in accordance with Türkiye's national action plan.

The promotion of biological control practices has gained increasing attention in research on alternative pest management strategies, aiming both to support biodiversity and to implement more sustainable control methods in agricultural fields. Among alternative control strategies, biological control has attracted the most attention. Biopesticides used in biological control are considered a safer, more sustainable, and potentially more cost-effective approach in the long term, both for the environment and human health (Uygun et al., 2016; van Lenteren, 2000).

Biopesticides can address the global need for new alternatives to chemical pesticides by managing and preventing resistance encountered by farmers and consumers, enhancing biodiversity, reducing carbon footprints, aiding in the management of chemical residues, and meeting farmers' productivity expectations (Marrone, 2024). Biopesticides are chemicals derived from natural sources, including bacteria, fungi, viruses, plants, animals, and minerals, used to suppress pest populations (Thakore, 2006).

Plant extracts and oils can be utilized as biopesticides against this disease, which is also defined as white mold in sunflower. Certain plant extracts or essential oils may enhance plant resistance to diseases or inhibit the growth of pathogens. Garlic (*Allium sativum* L.), a species of Asian origin belonging to the Alliaceae family, is a medicinal plant widely used in the treatment of various human diseases, including infections, cancer prevention, and the reduction of blood pressure and cholesterol levels. In addition, it exhibits antifungal, antihelminthic, antihypertensive, mild hypotensive, antidiabetic, antioxidant, and hepatoprotective properties (Cavalcanti et al., 2020). Moreover, in order to prevent white mold disease caused by *Sclerotinia sclerotiorum*, many oilseed producers prefer to advance the planting date of garlic (Pinto et al., 2000).

The antimicrobial activity of garlic was first described nearly 70 years ago, after which the chemical structure and properties of allicin were elucidated through a series of

publications by researchers at The Winthrop Chemical Company. More recent analyses have revealed that allicin accounts for approximately 75% of the sulfinates derived from garlic. Among more than 600 *Allium* species, the aqueous extracts of garlic—particularly rich in allicin-have attracted the greatest scientific attention (Wallock-Richards et al., 2014).

The mechanisms by which the compounds present in garlic extract (Table 1) inhibit or kill bacteria remain unclear. It is known, however, that allicin and other thiosulfinates can react with cysteine, thereby abolishing antimicrobial activity, and inhibit acetyl-CoA synthetases in plants, yeasts, and mammals (Focke et al., 1990). Most previous studies on the antibacterial activity of garlic extracts have focused on Escherichia coli and *Staphylococcus aureus*. In garlic extracts derived from oil, ajoene—an allyl sulfide derivative of allicin that is soluble in lipids—has been reported to cause broad-spectrum inhibition of microbial growth (Ishikawa et al., 1996).

Table 1. Bioactive compounds ıdentified in garlic extract

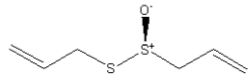 **Allicin**	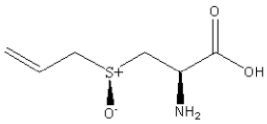 **Alliin**	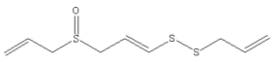 **Ajoene**
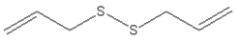 **Diallyl disulfide**	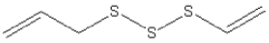 **Diallyl trisulfide**	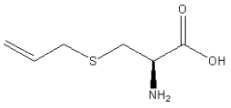 **S-Allylcysteine**
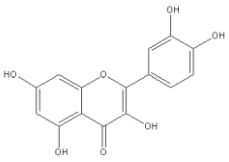 **Quercetin**	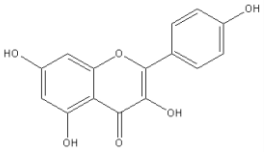 **Kaempferol**	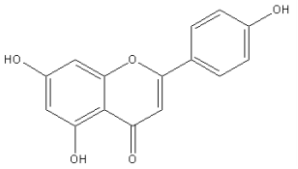 **Apigenin**

Experimental studies in the literature have demonstrated the efficacy of garlic against white mold disease caused by *Sclerotinia sclerotiorum*. The foundations of this research date back to 1978. In a study conducted that year, aqueous garlic leaf extract was tested on two pathogens: *Fusarium oxysporum* f. sp. *ciceris*, which causes wilt disease in *Cicer arietinum*, and *Sclerotinia sclerotiorum*. Seeds sown in pathogen-infested soil were treated with the extract, either individually or in combination, resulting in the production of non-wilted seedlings,

whereas all seedlings derived from untreated seeds exhibited symptoms of wilt. The study suggested the potential use of garlic leaf extract for controlling plant diseases under field conditions.

In 2017, an experimental study evaluated the effectiveness of three botanicals against *Sclerotinia sclerotiorum*, one of which was garlic extract. The results indicated that all three selected botanicals, including garlic extract, significantly inhibited fungal growth (Singh et al., 1979).

In a study conducted in 2019, a series of experimental approaches suggested that natural or environmentally friendly products, such as cow urine and garlic bulb extracts, could be utilized for the development of an Integrated Disease Management (IDM) module. This module aims to provide a safe, chemical-free, eco-friendly, and cost-effective strategy for the future management of white mold disease (Upadhyay & Tewari, 2019).

According to a study conducted in 2020, neem oil, garlic extract, castor oil, cow urine, hing powder, and turmeric powder were tested against the *Sclerotinia sclerotiorum* pathogen using the poisoned food technique. Among the six materials, garlic extract was found to be the most effective in inhibiting mycelial growth of *Sclerotinia sclerotiorum* (69.71%, 95.72%, and 98.00%). The study further demonstrated that all three concentrations of garlic extract (5%, 10%, and 15%) were effective in reducing the incidence of white mold disease (Bairwa et al., 2020).

In another study conducted in 2020, the aim was to identify potential bacteria and yeasts capable of preventing *Sclerotinia sclerotiorum* infection in garlic through biocontrol. Two yeasts (*Pichia kudriavzevii* and *Candida labiduridarum*) and four bacteria (*Bacillus acidiceler*, *B. macauensis*, *B. amyloliquefaciens*, and *B. pumilus*) were tested. The effects of volatile and diffusible antifungal metabolites on in vitro mycelial growth of *S. sclerotiorum* were evaluated. Garlic cloves were immersed in a suspension of each microorganism (1×10^8 cells mL^{-1}) and maintained in a humid chamber for 15 days. The results showed that the growth of *S. sclerotiorum* in garlic was more strongly inhibited by volatile metabolites produced by *C. labiduridarum*, *B. macauensis*, *B. amyloliquefaciens*, and *B. pumilus* than by other tested agents, with inhibition rates ranging from 74.61% to 87.61% (Cavalcanti et al., 2020).

Despite the numerous experimental studies on garlic extract, no studies have been reported in the literature in which all compounds were isolated to specifically identify the active components and elucidate the inhibition mechanisms.

Nowadays, the necessity to implement alternative methods that eliminate the adverse effects of chemical control against diseases, which reduce crop yield, has become evident. One such approach involves plant-derived products. The diverse range of compounds present in plant extracts can play a role in enhancing crop resistance against various diseases and pests (Torun et al., 2023). In this study, the inhibitory potential of compounds present in garlic extract—commonly applied for antibacterial purposes—against the *Sclerotinia sclerotiorum* pathogen, which causes white mold disease, was investigated in silico using molecular docking. The ability of these compounds to inhibit the pathogen was assessed through docking studies, and the results revealed that quercetin, kaempferol, and apigenin, present in the natural extract, have potential as biopesticides. Furthermore, based on the chemical properties of these compounds, the effects of functional groups in chemical structures were discussed in the context of producing environmentally and human health-friendly biopesticides, with consideration of sustainable agriculture and food safety.

The methods of this study included molecular modeling and docking analyses. The effects of compounds present in garlic extract (such as allicin, alliin, ajoene, sulfur-containing compounds, and flavonoids) on the protein structure of the white mold pathogen were investigated using a computer-based modeling approach. These analyses allowed the observation of interactions between the compounds and pathogen cells.

Software tools such as Gaussian09 and Discovery Studio were employed to characterize these interactions during molecular modeling. Gaussian09 was used to optimize the compounds and prepare them for docking studies. Docking analyses were performed using the AutoDock Vina program, which was applied to predict the binding affinities of the compounds to the pathogen’s protein structure.

The outputs obtained from this study may contribute to the development of environmentally friendly practices, food safety, and sustainable agricultural strategies.

2. MATERIALS AND METHODS

2.1. Optimization of Garlic Extract Compounds

Gaussian09 is a software designed to perform calculations based on the fundamental principles of quantum mechanics to model molecular systems under a wide range of conditions. Gaussian is widely used in established and emerging areas of chemistry research to study molecules and reactions that are difficult or impossible to examine experimentally, including both known and potential species and compounds.

GaussView 5.0.8 is a graphical user interface designed to prepare input files for Gaussian programs and to visualize Gaussian output data. GaussView allows molecules to be rendered visually, enabling rotation, translation, and modification of molecular structures. It also facilitates the preparation of input files even for complex calculations and allows graphical examination of results computed by the Gaussian program (Frisch, 2009).

Within the scope of the "Optimization of Garlic Extract Compounds" study, the structures of ajoene, alliin, allicin, apigenin, diallyl disulfide, diallyl trisulfide, kaempferol, quercetin, and S-allylcysteine were optimized in the gas phase using the Gaussian09 program at the DFT/B3LYP/6-31++G(d,p) level of theory. The purpose of optimization is to ensure that the molecules to be used in docking studies adopt the most stable conformations. Three-dimensional representations of the garlic extract compounds after optimization calculations are presented in Table 2.

Table 2. 3D Structures of optimized garlic extract compounds

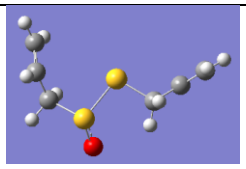 Allicin	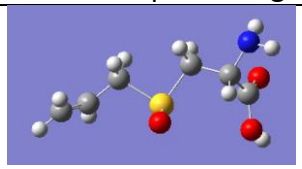 Alliin	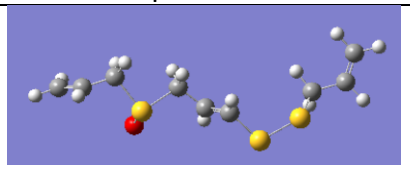 Ajoene
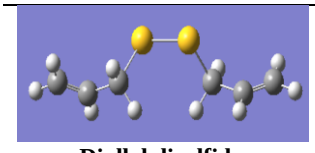 Diallyl disulfide	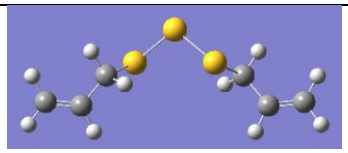 Diallyl trisulfide	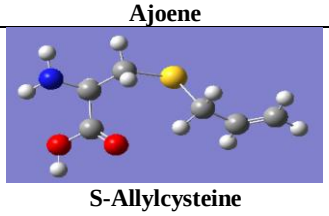 S-Allylcysteine
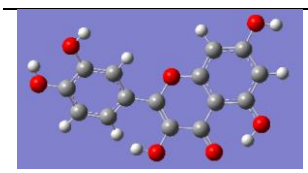 Quercetin	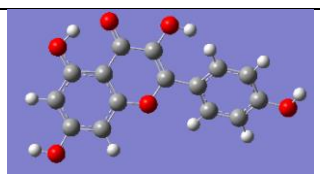 Kaempferol	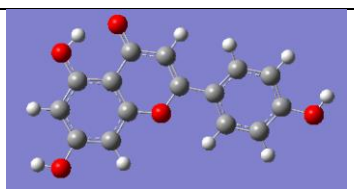 Apigenin

2.2. Selection of the Solved Pathogen Structure from Databases for Docking

The Protein Data Bank (PDB) is a comprehensive repository of three-dimensional structures of large biological molecules, such as proteins and nucleic acids. The structural information available in the PDB is primarily obtained through X-ray crystallography or nuclear magnetic resonance (NMR) spectroscopy. Researchers can access the structural data submitted to the PDB by biologists and biochemists from around the world (Berman et al., 2000).

Macromolecules in the Protein Data Bank are stored as files with the .pdb extension. Each PDB file is identified by a four-character code, the first of which is a digit. The .pdb format contains atomic coordinates of the macromolecule, as well as information on its primary and secondary structures, crystallographic structure factors, and NMR data. The PDB format is recognized by virtually all software used in drug design.

The resolved pathogen structure with the PDB code 2X2T was selected from the RCSB database based on criteria such as resolution, presence of mutations, and year of crystallization. Additional reasons for choosing this structure include that 2X2T represents SSA (Sclerotinia sclerotiorum Agglutinin), a lectin protein from *Sclerotinia sclerotiorum*. Lectins are known for their carbohydrate-binding properties and play a critical role in various biological processes, particularly in infection and cell adhesion mechanisms in pathogens. The 2X2T protein facilitates the binding of the pathogen to plant cells, playing a key role in the early stages of infection. These proteins are located on the pathogen's surface and directly interact with the plant surface. Therefore, targeting this protein with an antifungal agent may effectively halt the infection process at an early stage (Sulzenbacher et al., 2010).

Table 3. Resolved pathogen structures from the RCSB database

PDB Code	Resource	Mutation	Resolution	Method	Year	Ligand	Definition
2X2S	Sclerotinia sclerotiorum	-	1.60 A^0	X-Ray	2010	GOL	Crystal structure of Sclerotinia sclerotiorum agglutinin SSA
2X2T	Sclerotinia sclerotiorum	-	1.97 A^0	X-Ray	2010	PG4, SO4, beta-D-galactopyranose-(1-3)-2-acetamido-2-deoxy-beta-D-galactopyranose	CRYSTAL STRUCTURE OF SCLEROTINIA SCLEROTIORUM AGGLUTININ SSA in complex with Gal-beta1,3-Galnac
2FBW	Gallus gallus	-	2.06 A^0	X-Ray	2005	FAD, HEM, UMQ, SF4, BOG,CBE, FES, Y3P, GOL, AZI, K, NA, UNL	Avian respiratory complex II with carboxin bound
2Y9W	Agaricus bisporus	-	2.30 A^0	X-Ray	2011	HO, PGE, PEG, CU	Crystal structure of PPO3, a tyrosinase from Agaricus bisporus, in deoxy-form

Allicin, the main component of garlic extracts, along with other sulfur-containing compounds, can react with thiol groups on protein surfaces. Lectins, which are generally surface-exposed proteins mediating ligand binding, thus serve as suitable targets for such interactions. The carbohydrate-binding regions of 2X2T were selected as docking targets because garlic compounds may bind to these regions and inhibit protein function. According to literature reports, the disaccharide Gal-β1,3-GalNAc (T-antigen) is considered the natural ligand that binds to the active site of the protein. PG4 and SO4 may be present as solvent additives during crystallization and may not bind directly to the active site [32].

Sclerotinia sclerotiorum is a key pathogen in white mold disease, and lectin proteins play a critical role during the early stages of infection in plants. Moreover, the selected 2X2T resolved protein structure, being specific to *Sclerotinia sclerotiorum*, provides a focused target for biopesticide development studies.

2.3. Validation of the AutoDock Vina Program

The validation of the docking method is performed by removing the ligand present in the enzyme's X-ray structure and re-docking it into the same enzyme using a docking program, followed by evaluating the deviation of the resulting conformations from the reference structure. In the present study, the ligand "beta-D-galactopyranose-(1-3)-2-acetamido-2-

deoxy-beta-D-galactopyranose" within the 2X2T structure was used for validation. The ligand, after being removed from the enzyme, was re-docked into its binding site of the 2X2T enzyme using the AutoDock Vina program.

Firstly, all water molecules, PG4 (tetraethylene glycol), and the SO4 sulfate ion present in the 2X2T structure were removed using the ADT user interface. The ligand "beta-D-galactopyranose-(1-3)-2-acetamido-2-deoxy-beta-D-galactopyranose" was then separated from the 2X2T structure, again using the ADT interface. A configuration file was prepared using Cartesian coordinates of 40 × 40 × 40 (x = 2.991, y = -18.685, z = 8.008), and the docking procedure was performed. The RMSD value of the ligand conformation showing the best fit was found to be 1.624 Å. Since the RMSD value is below 2 Å, the AutoDock Vina program was deemed suitable for the selected system (Keşkek Karabulut et al., 2024). Figure 3 shows the overlap of the best post-docking conformation of the ligand with its initial state.

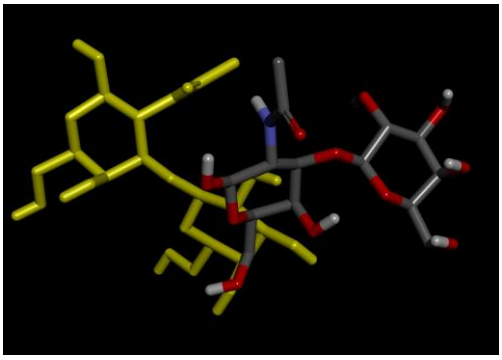

Figure 3. Superimposition of the ligand after re-docking

2.4. Preparation of Ligands for Docking Studies

After optimization of the garlic extract components using the Gaussian09 program, the resulting .log files were converted to the .pdb file format for use in docking calculations, and these structures were employed in the docking analyses. Using ADT Tools, the opened ligand files were first analyzed to determine the torsional root and the number of torsions in each ligand molecule. Finally, the prepared ligand structures were saved in the .pdbqt format, making them ready for the docking procedure.

3. RESULTS

3.1. Molecular Docking Studies

To perform docking using AutoDock Vina, a configuration file was created via the ADT interface, containing the enzyme and ligand files in .pdbqt format. This file includes parameters specifying the names and formats of the pathogen and ligand files (garlic extract components), the Cartesian coordinates of the target site, and the dimensions of the docking area. Additionally, the Cartesian coordinates and size of the grid box for the docking grid map are defined in this file. A configuration file was prepared using Cartesian coordinates of 40 × 40 × 40 (x = 2.991, y = -18.685, z = 8.008). After preparing the ligands and macromolecules, the configuration file serves as the sole input for AutoDock Vina during calculations. The program also generates a log and output file in .pdbqt format for each garlic extract component. Table 4 presents the generated log files.

Table 4. Docking .log files of garlic extract components

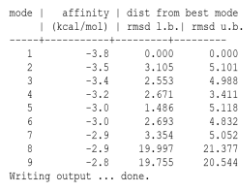

mode	affinity (kcal/mol)	dist from best mode rmsd l.b.	rmsd u.b.
1	-3.8	0.000	0.000
2	-3.5	3.105	5.101
3	-3.4	2.553	4.988
4	-3.2	2.671	3.411
5	-3.0	1.486	5.118
6	-3.0	2.693	4.832
7	-2.9	3.354	5.052
8	-2.9	19.997	21.377
9	-2.8	19.755	20.544

Writing output ... done.

Allicin

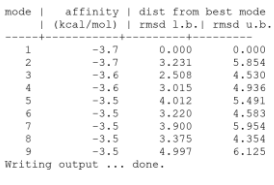

mode	affinity (kcal/mol)	dist from best mode rmsd l.b.	rmsd u.b.
1	-3.7	0.000	0.000
2	-3.7	3.231	5.854
3	-3.6	2.508	4.530
4	-3.6	3.015	4.936
5	-3.5	4.012	5.491
6	-3.5	3.220	4.583
7	-3.5	3.900	5.954
8	-3.5	3.375	4.354
9	-3.5	4.997	6.125

Writing output ... done.

Alliin

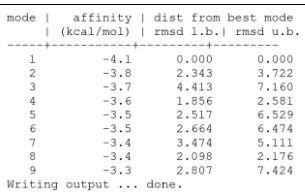

mode	affinity (kcal/mol)	dist from best mode rmsd l.b.	rmsd u.b.
1	-4.1	0.000	0.000
2	-3.8	2.343	3.722
3	-3.7	4.413	7.160
4	-3.6	1.856	2.581
5	-3.5	2.517	6.529
6	-3.5	2.664	6.474
7	-3.4	3.474	5.111
8	-3.4	2.098	2.176
9	-3.3	2.807	7.424

Writing output ... done.

Ajoene

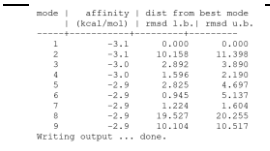

mode	affinity (kcal/mol)	dist from best mode rmsd l.b.	rmsd u.b.
1	-3.1	0.000	0.000
2	-3.1	10.158	11.398
3	-3.0	2.892	3.890
4	-3.0	1.596	2.190
5	-2.9	2.825	4.697
6	-2.9	0.945	5.137
7	-2.9	1.224	1.604
8	-2.9	19.527	20.255
9	-2.9	10.104	10.517

Writing output ... done.

Diallyl disulfide

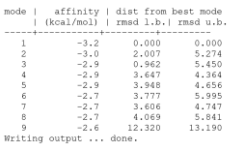

mode	affinity (kcal/mol)	dist from best mode rmsd l.b.	rmsd u.b.
1	-3.2	0.000	0.000
2	-3.0	2.007	5.274
3	-2.9	0.962	5.450
4	-2.9	3.647	4.364
5	-2.9	3.948	4.656
6	-2.7	3.777	5.995
7	-2.7	3.606	4.747
8	-2.7	4.069	5.841
9	-2.6	12.320	13.190

Writing output ... done.

Diallyl trisulfide

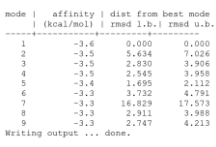

mode	affinity (kcal/mol)	dist from best mode rmsd l.b.	rmsd u.b.
1	-3.6	0.000	0.000
2	-3.5	5.634	7.026
3	-3.5	2.830	3.906
4	-3.5	2.545	3.958
5	-3.4	1.695	2.112
6	-3.3	3.732	4.791
7	-3.3	16.829	17.573
8	-3.3	2.911	3.988
9	-3.3	2.747	4.213

Writing output ... done.

S-Allylcysteine

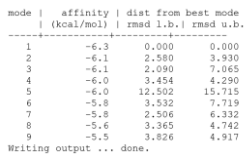

mode	affinity (kcal/mol)	dist from best mode rmsd l.b.	rmsd u.b.
1	-6.3	0.000	0.000
2	-6.1	2.580	3.930
3	-6.1	2.090	7.065
4	-6.0	3.454	4.290
5	-6.0	12.502	15.715
6	-5.8	3.532	7.719
7	-5.8	2.506	6.332
8	-5.6	3.365	4.742
9	-5.5	3.826	4.917

Writing output ... done.

Quercetin

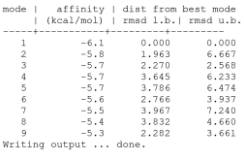

mode	affinity (kcal/mol)	dist from best mode rmsd l.b.	rmsd u.b.
1	-6.1	0.000	0.000
2	-5.8	1.963	6.667
3	-5.7	2.270	2.568
4	-5.7	3.645	6.233
5	-5.7	3.786	6.474
6	-5.6	2.766	3.937
7	-5.5	3.967	7.240
8	-5.4	3.832	4.660
9	-5.3	2.282	3.661

Writing output ... done.

Kaempferol

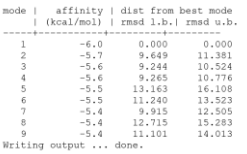

mode	affinity (kcal/mol)	dist from best mode rmsd l.b.	rmsd u.b.
1	-6.0	0.000	0.000
2	-5.7	9.649	11.381
3	-5.6	9.244	10.524
4	-5.6	9.265	10.776
5	-5.5	13.163	16.108
6	-5.5	11.240	13.523
7	-5.4	9.915	12.505
8	-5.4	12.715	15.283
9	-5.4	11.101	14.013

Writing output ... done.

Apigenin

3.2. Docking Analysis of Allicin

Docking of the allicin molecule prepared in .pdbqt format with the 2X2T pathogen structure, prepared for docking, was performed using the AutoDock Vina program, employing the Cartesian coordinates used in the validation. The docking calculation yielded nine possible conformations, with the best-binding conformation exhibiting a binding energy of -3.8 kcal/mol. The interactions within the binding site were analyzed using ADT Tools and Discovery Studio. The 2D and 3D representations of the binding mode are shown in Figure 4.

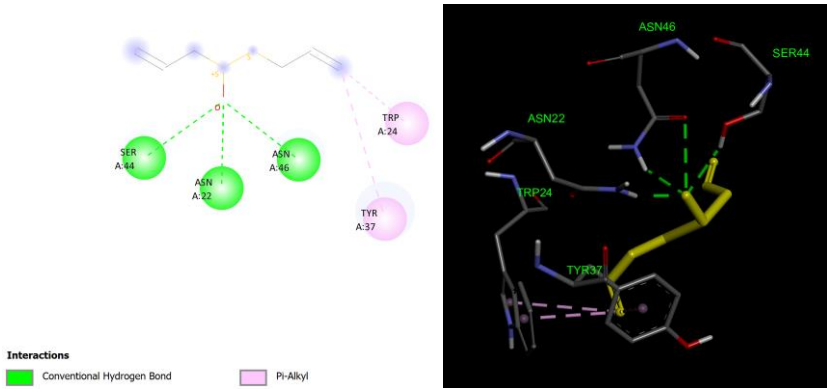

Figure 4. Allicin binding in the active site (2D and 3D views)

Analysis of the binding position within the active site revealed the presence of three hydrogen bonds with the amino acid residues ASN22, SER44, and ASN46. Additionally, pi-alkyl interactions were observed with the residues TRP24 and TYR37.

3.3. Docking Analysis of Alliin

Docking of the alliin molecule, prepared in .pdbqt format, with the 2X2T pathogen structure ready for docking was performed using the AutoDock Vina program, employing the Cartesian coordinates used in the validation. The docking calculation produced nine possible conformations, with the best-binding conformation exhibiting a binding energy of -3.7 kcal/mol. Interactions within the binding site were analyzed using ADT Tools and Discovery Studio. The 2D and 3D representations of the binding mode are shown in Figure 5.

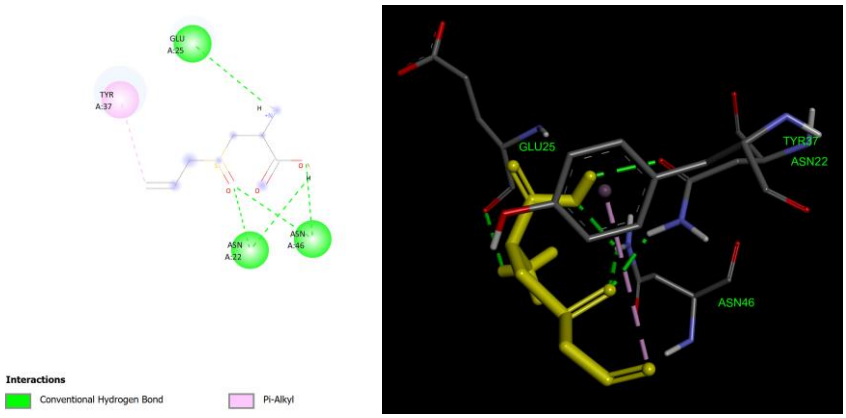

Figure 5. Alliin binding in the active site (2D and 3D views)

Analysis of the binding position within the active site revealed the presence of five hydrogen bonds with the amino acid residues ASN22, GLU25, and ASN46. Additionally, a pi-alkyl interaction was observed with the residue TYR37.

3.4. Docking Analysis of Ajoene

Docking of the ajoene molecule, prepared in .pdbqt format, with the 2X2T pathogen structure ready for docking was performed using the AutoDock Vina program, employing the Cartesian coordinates used in the validation. The docking calculation generated nine possible conformations, with the best-binding conformation exhibiting a binding energy of -4.1 kcal/mol. Interactions within the binding site were analyzed using ADT Tools and Discovery Studio. The 2D and 3D representations of the binding mode are shown in Figure 6.

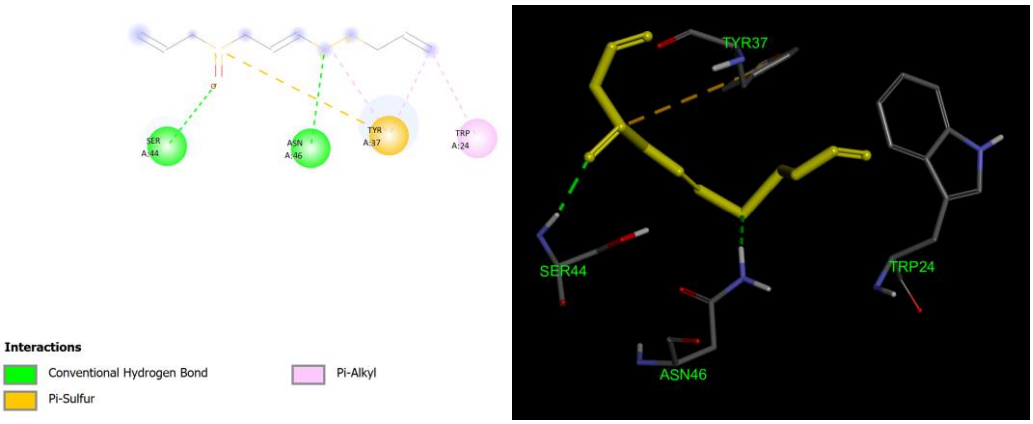

Figure 6. Ajoene Binding in the active site (2D and 3D views)

Analysis of the binding position within the active site revealed the presence of two hydrogen bonds with the amino acid residues SER44 and ASN46. Additionally, pi-alkyl interactions were observed with TYR37 and TRP24. Furthermore, a pi-sulfur interaction was also detected with TYR37.

3.5. Docking Analysis of Diallyl Disulfide

Docking of the diallyl disulfide molecule, prepared in .pdbqt format, with the 2X2T pathogen structure ready for docking was performed using the AutoDock Vina program, employing the Cartesian coordinates used in the validation. The docking calculation generated nine possible conformations, with the best-binding conformation exhibiting a binding energy of -3.1 kcal/mol. Interactions within the binding site were analyzed using ADT Tools and Discovery Studio. The 2D and 3D representations of the binding mode are shown in Figure 7.

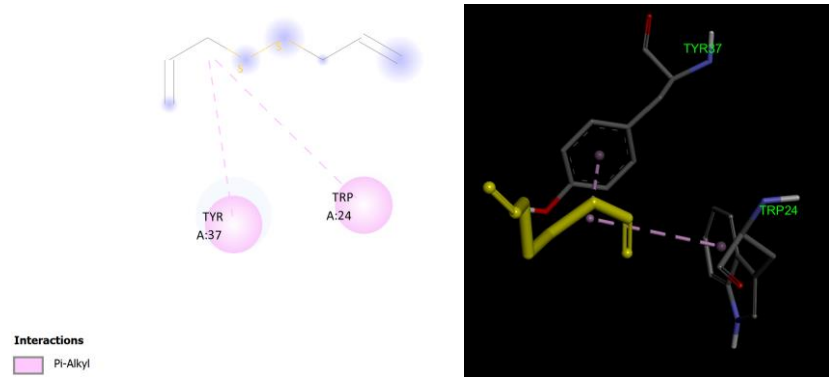

Figure 7. Diallyl disulfide binding in the active site (2D and 3D views)

Analysis of the binding position within the active site revealed the presence of pi-alkyl interactions with the amino acid residues TYR37 and TRP24.

3.6. Docking Analysis of Diallyl Trisulfide

Docking of the diallyl trisulfide molecule, prepared in .pdbqt format, with the 2X2T pathogen structure ready for docking was performed using the AutoDock Vina program, employing the Cartesian coordinates used in the validation. The docking calculation produced nine possible conformations, with the best-binding conformation exhibiting a binding energy of -3.2 kcal/mol. Interactions within the binding site were analyzed using ADT Tools and Discovery Studio. The 2D and 3D representations of the binding mode are shown in Figure 8.

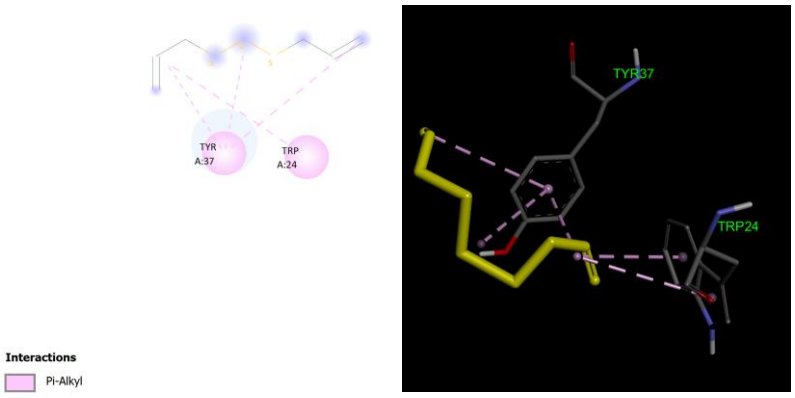

Figure 8. Diallyl trisulfide binding in the active site (2D and 3D views)

Analysis of the binding position within the active site revealed the presence of pi-alkyl interactions with the amino acid residues TYR37 and TRP24.

3.7. Docking Analysis of S-Allylcysteine

Docking of the S-allylcysteine molecule, prepared in .pdbqt format, with the 2X2T pathogen structure ready for docking was performed using the AutoDock Vina program, employing the Cartesian coordinates used in the validation. The docking calculation produced nine possible conformations, with the best-binding conformation exhibiting a binding energy of -3.6 kcal/mol. Interactions within the binding site were analyzed using ADT Tools and Discovery Studio. The 2D and 3D representations of the binding mode are shown in Figure 9.

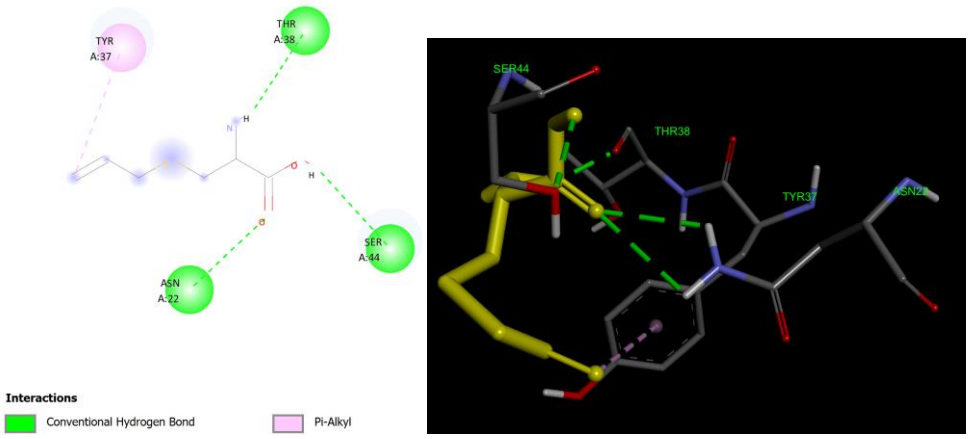

Figure 9. S-Allylcysteine binding in the active site (2D and 3D views)

Analysis of the binding position within the active site revealed the presence of three hydrogen bonds with the amino acid residues SER44, THR38, and ASN22. Additionally, a pi-alkyl interaction was observed with the residue TYR37.

3.8. Docking Analysis of Quercetin

Docking of the quercetin molecule, prepared in .pdbqt format, with the 2X2T pathogen structure ready for docking was performed using the AutoDock Vina program, employing the Cartesian coordinates used in the validation. The docking calculation generated nine possible conformations, with the best-binding conformation exhibiting a binding energy of -6.3 kcal/mol. Interactions within the binding site were analyzed using ADT Tools and Discovery Studio. The 2D and 3D representations of the binding mode are shown in Figure 10.

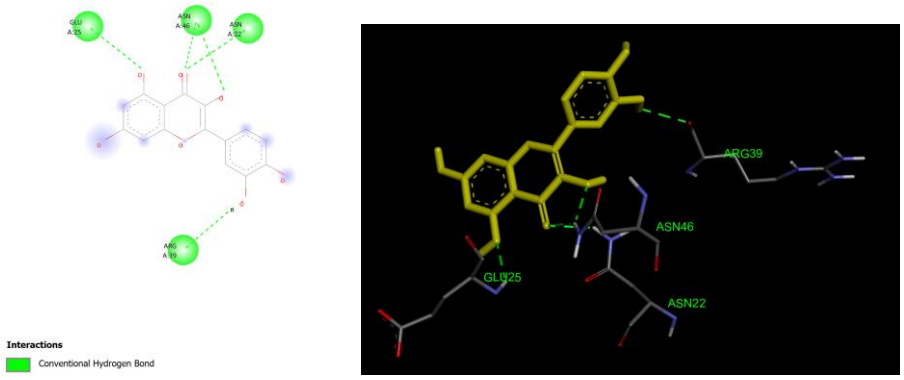

Figure 10. Quercetin binding in the active site (2D and 3D views)

Analysis of the binding position within the active site revealed the presence of four hydrogen bonds with the amino acid residues GLU25, ASN46, ASN22, and ARG39.

3.9. Docking Analysis of Kaempferol

Docking of the kaempferol molecule, prepared in .pdbqt format, with the 2X2T pathogen structure ready for docking was performed using the AutoDock Vina program, employing the Cartesian coordinates used in the validation. The docking calculation generated nine possible conformations, with the best-binding conformation exhibiting a binding energy of -6.1 kcal/mol. Interactions within the binding site were analyzed using ADT Tools and Discovery Studio. The 2D and 3D representations of the binding mode are shown in Figure 11.

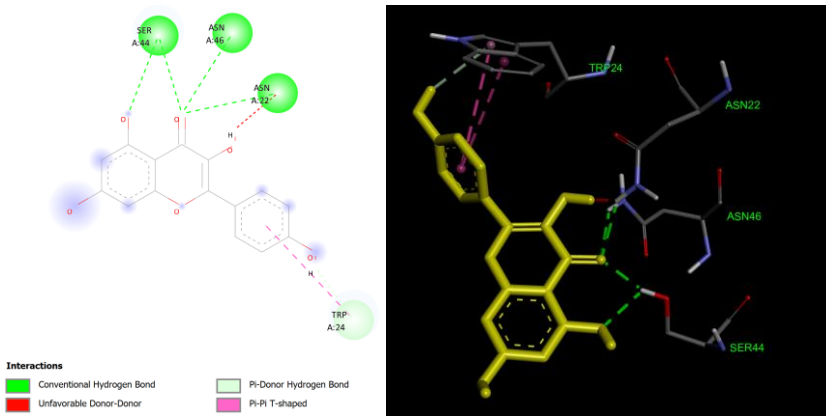

Figure 11. Kaempferol binding in the active site (2D and 3D views)

Analysis of the binding position within the active site revealed the presence of four hydrogen bonds with the amino acid residues SER44, ASN46, and ASN22. Additionally, pi-donor hydrogen bonding and pi–pi interactions were observed with the residue TRP24. Furthermore, undesired donor–donor interactions were detected with ASN22.

3.10. Docking Analysis of Apigenin

Docking of the apigenin molecule, prepared in .pdbqt format, with the 2X2T pathogen structure ready for docking was performed using the AutoDock Vina program, employing the Cartesian coordinates used in the validation. The docking calculation generated nine possible conformations, with the best-binding conformation exhibiting a binding energy of -6.0 kcal/mol. Interactions within the binding site were analyzed using ADT Tools and Discovery Studio. The 2D and 3D representations of the binding mode are shown in Figure 12.

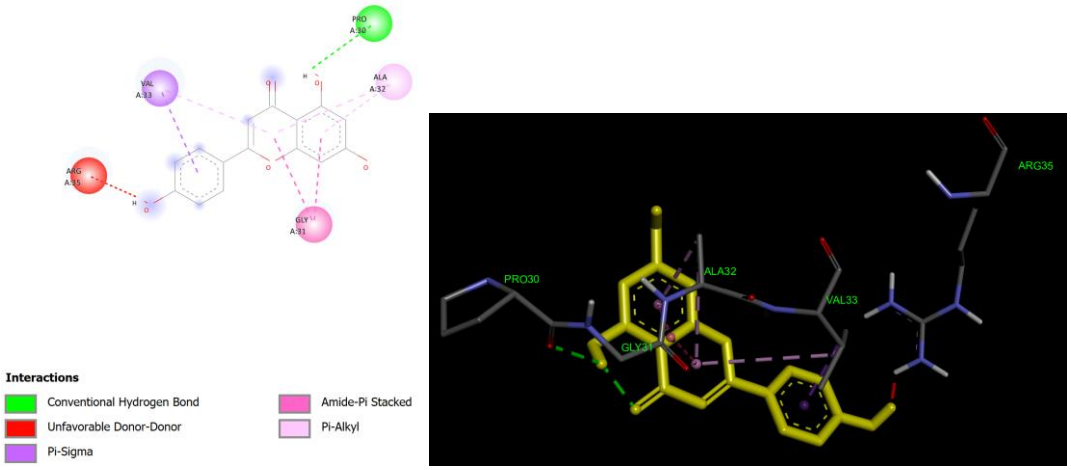

Figure 12. Apigenin binding in the active site (2D and 3D views)

Analysis of the binding position within the active site revealed the presence of a hydrogen bond with the amino acid residue PRO30. Pi–sigma interactions were observed with VAL33, and amid–pi stacking interactions were detected with GLY31. Additionally, pi-alkyl interactions were identified with the residues VAL33 and ALA32.

4. DİSCUSSİON

Table 5. Binding energies and ınteractions of garlic extract components

Garlic Extract	Molecular Structure	Binding Energy (kcal/mol)	Binding Interactions
Allicin	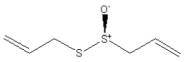	-3.8	• Three hydrogen bonds with the amino acid residues ASN22, SER44, and ASN46 • Pi–alkyl interactions with the residues TRP24 and TYR37
Alliin	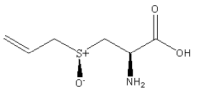	-3.7	• Five hydrogen bonds with the amino acid residues ASN22, GLU25, and ASN46 • Pi–alkyl interactions with the residue TYR37
Ajoene	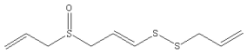	-4.1	• Two hydrogen bonds with the amino acid residues SER44 and ASN46 • Pi–alkyl interactions with the residues TYR37 and TRP24 • Pi–sulfur interaction with the residue TYR37
Diallyl Disulfide	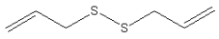	-3.1	• Pi–alkyl interactions with the amino acid residues TYR37 and TRP24
Diallyl Trisulfide	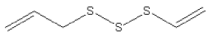	-3.2	• Pi–alkyl interactions with the amino acid residues TYR37 and TRP24
S-Allylcysteine	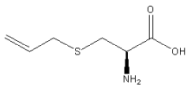	-3.6	• Three hydrogen bonds with the amino acid residues SER44, THR38, and ASN22 • Pi–alkyl interaction with the residue TYR37
Quercetin	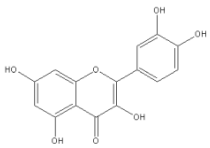	-6.3	• Four hydrogen bonds with the amino acid residues GLU25, ASN46, ASN22, and ARG39
Kaempferol		-6.1	• Four hydrogen bonds with the amino acid residues SER44, ASN46, and ASN22

	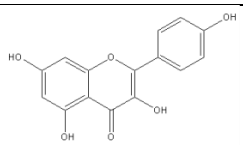		• Pi-donor hydrogen bond and pi–pi interaction with the residue TRP24
Apigenin	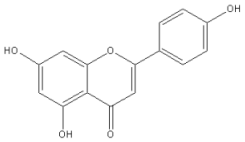	-6.0	• Hydrogen bond with the amino acid residue PRO30 • Pi–sigma interaction with the residue VAL33 • Amid–pi stacking interaction with the residue GLY31 • Pi–alkyl interactions with the residues VAL33 and ALA32

Based on the docking studies conducted in this study, the flavonoid compounds present in garlic extract—quercetin, kaempferol, and apigenin—demonstrated potential as biopesticides. Compared to other compounds in the extract, the flavonoid group exhibited stronger binding to the pathogen's active site and more favorable interactions within this region. These results indicate that quercetin, kaempferol, and apigenin possess a higher capacity to inhibit the pathogen.

When the garlic extract compounds are ranked according to their inhibitory potential, from the highest to the lowest binding affinity, the order is as follows:

Quercetin > Kaempferol > Apigenin > Ajoene > Allicin > Alliin > S-Allylcysteine > Diallyl Trisulfide > Diallyl Disulfide

Based on the docking results obtained in this study (binding energies) and the interactions observed within the active site, an analysis of the functional groups and molecular structures indicates that:

- The presence of sulfur reduces the pesticidal activity and the potential to inhibit the pathogen.
- Conversely, an increase in the number and branching of carbon atoms in the molecular structure positively influences pesticidal activity and pathogen inhibition potential, despite the presence of sulfur.
- The presence of a benzene ring in the molecular structure positively affects pesticidal activity and pathogen inhibition potential.
- The presence of hydroxyl groups (-OH) in the molecular structure also enhances pesticidal activity and the potential to inhibit the pathogen.

These findings can serve as supportive molecular-level insights for the design of environmentally friendly and sustainable pesticides.

Conflict of Interest

There is no conflict of interest with any institution or person in the study.

Acknowledgments

This article was supported by the Kırklareli University Scientific Research Projects Coordination Unit (KLÜBAP) under the project numbered KLÜBAP-278, titled “Investigation of Biopesticide Properties of Garlic Extract Compounds Suitable for Sustainable Agriculture and Food Safety against White Mold Disease in Sunflower Production”.

5. REFERENCES

Bairwa, V. K., Godika, S., Sharma, J., Nayak, R. K., Gahlot, N., & Choudhary, S. (2020). Management of sclerotinia rot disease of brinjal (*Sclerotinia sclerotiorum* Lib.) through indigenous materials under in vitro and in vivo conditions. *International Journal of Chemical Studies, 8*(4), 881–885.

Berman, H. M., Westbrook, J., Feng, Z., Gilliland, G., Bhat, T. N., Weissig, H., & Bourne, P. E. (2000). The Protein Data Bank. *Nucleic Acids Research, 28*(1), 235–242.

Bolton, M. D., Thomma, B. P., & Nelson, B. D. (2006). *Sclerotinia sclerotiorum* (Lib.) de Bary: Biology and molecular traits of a cosmopolitan pathogen. *Molecular Plant Pathology, 7*(1), 1–16.

Cavalcanti, V. P., Araújo, N. A. F., Machado, N. B., Júnior, P. S. P. C., Pasqual, M., Alves, E., & Doria, J. (2020). Yeasts and *Bacillus* spp. as potential biocontrol agents of *Sclerotinia sclerotiorum* in garlic. *Scientia Horticulturae, 261*, 108931.

Ecer, K., Güner, O., & Çetin, M. (2021). Avrupa Yeşil Mutabakatı ve Türkiye ekonomisinin uyum politikaları. *İşletme ve İktisat Çalışmaları Dergisi, 9*(2), 125–144.

Focke, M., Feld, A., & Lichtenthaler, H. K. (1990). Allicin, a naturally occurring antibiotic from garlic, specifically inhibits acetyl-CoA synthetase. *FEBS Letters, 261*(1), 106–108.

Frisch, A. (2009). *Gaussian 09W reference* (25 p., 470). Wallingford, USA: Gaussian, Inc.

Gulya, T. J., Harveson, R., Mathew, F., Block, C., Thompson, S., Kandel, H., Berglund, D., Sandbakken, J., Kleingartner, L., & Markell, S. (2019). Comprehensive disease survey of U.S. sunflower: Disease trends, research priorities and unanticipated impacts. *Plant Disease, 103*(4), 601–618.

Gyanwali, P., Khanal, R., Pokharel, N. P., Tharu, B., Koirala, R., Paudel, S., & Paudel, R. (2023). In vitro analysis of antifungal effects of botanicals on *Sclerotinia sclerotiorum* causing white mold disease. *Agriculture and Food Sciences Research, 10*(2), 8–13.

Harveson, R. M. (2011). Sclerotinia diseases of sunflower in Nebraska. *NebGuide*, University of Nebraska–Lincoln Extension, Institute of Agriculture and Natural Resources. http://www.ianrpubs.unl.edu/pages/publicationD.jsp

Hegedus, D. D., & Rimmer, S. R. (2005). *Sclerotinia sclerotiorum*: When ‘to be or not to be’ a pathogen? *FEMS Microbiology Letters, 251*(2), 177–184.

Ishikawa, K., Naganawa, R., Yoshida, H., Iwata, N., Fukuda, H., Fujino, T., & Suzuki, A. (1996). Antimutagenic effects of ajoene, an organosulfur compound derived from garlic. *Bioscience, Biotechnology, and Biochemistry, 60*(12), 2086–2088.

Keşkek Karabulut, Y., Yiğit, A., Karacalı Tunç, A., Saritaş, B. M., Kesici, S., Uzun, Y., & Sadullahoğlu, C. (2024). MAO-A inhibitor properties by molecular modeling method, antimicrobial activity and characterization of silver nanoparticles synthesized from *Lactifluus bertillonii* mushroom. *Duzce University Journal of Science & Technology, 12*(4).

Koçak, R., & Boyraz, N. (2021). The incidence rate of white rot (Sclerotinia sclerotiorum (Lib.) de Bary) disease in sunflower cultivation areas in Konya and Aksaray provinces and its pathogenic potential. Selcuk Journal of Agriculture and Food Sciences, 35(2), 101–107.

Markell, S. G., Harveson, R. M., Block, C. C., & Gulya, T. J. (2015). Sunflower diseases. In *Sunflower* (pp. 93–128). AOCS Press.

Marrone, P. G. (2024). Status of the biopesticide market and prospects for new bioherbicides. *Pest Management Science, 80*(1), 81–86.

Möhring, N., Ingold, K., Kudsk, P., Martin-Laurent, F., Niggli, U., Siegrist, M., & Finger, R. (2020). Pathways for advancing pesticide policies. *Nature Food, 1*(9), 535–540.

Pinto, C. M. F., Maffia, L. A., Casali, V. W. D., Berger, R. D., & Cardoso, A. A. (2000). Production components and yield loss of garlic cultivars planted at different times in a field naturally infested with *Sclerotium cepivorum*. *International Journal of Pest Management, 46*(1), 67–72.

Schebesta, H., & Candel, J. J. (2020). Game-changing potential of the EU's Farm to Fork Strategy. *Nature Food, 1*(10), 586–588.

Semerci, A. (2019). Yağlık ayçiçeği üretiminin ekonomik analizi: Kırklareli ili örneği. *Türk Tarım ve Doğa Bilimleri Dergisi, 6*(4), 616–623.

Singh, U. P., Pathak, K. K., Khare, M. N., & Singh, R. B. (1979). Effect of leaf extract of garlic on *Fusarium oxysporum* f. sp. *ciceri*, *Sclerotinia sclerotiorum* and on gram seeds. *Mycologia, 71*(3), 556–564.

Presidency of Strategy and Budget. (2023, December). *Twelfth Development Plan 2024–2028*. https://www.sbb.gov.tr/wp-content/uploads/2023/12/On-Ikinci-Kalkinma-Plani_2024-2028_11122023.pdf

Sulzenbacher, G., Roig-Zamboni, V., Peumans, W. J., Rougé, P., Van Damme, E. J., & Bourne, Y. (2010). Crystal structure of the GalNAc/Gal-specific agglutinin from the phytopathogenic ascomycete *Sclerotinia sclerotiorum* reveals novel adaptation of a β-trefoil domain. *Journal of Molecular Biology, 400*(4), 715–723.

Süzer, S., & Çulhacı, E. (2017). Farklı organomineral ve inorganik kompoze gübrelerin kışlık ekmeklik buğday tane verimi ve bazı verim unsurları üzerine etkileri. *Toprak Bilimi ve Bitki Besleme Dergisi, 5*(2), 87–92.

Tan, A., & Kaya, Y. (2019). Sunflower (Helianthus annuus L.) genetic resources, production and researches in Turkey. *OCL-Oilseeds and fats, Crops and Lipids*, *26*(3).

Institute for Agricultural Economics and Policy Development. (2022, January). *Ayçiçeği, January 2022, Tarım Ürünleri Piyasa Raporu*. https://arastirma.tarimorman.gov.tr/tepge/Belgeler/PDF%20Tar%C4%B1m%20%C3%9Cr%C3%BCnleri%20Piyasalar%C4%B1/2022-Ocak%20Tar%C4%B1m%20%C3%9Cr%C3%BCnleri%20Rapor%C4%B1/Ay%C3%A7i%C3%A7e%C4%9Fi,%20Ocak-2022,%20Tar%C4%B1m%20%C3%9Cr%C3%BCnleri%20Piyasa%20Raporu--+.pdf

Thakore, Y. (2006). The biopesticide market for global agricultural use. *Industrial Biotechnology, 2*(3), 194–208.

Torun, E. Ö., Koçak, M. E., Kayra, B., Ercan, F., & Yalçın, S. (2023). *Galleria mellonella*'nın enzimatik savunma sistemi elemanları, glutatyon peroksidaz (GPx) ve glutatyon-S-transferaz (GST) enzimleri üzerine oktadekanoik asit, oleik asit ve n-hekzadekanoik asitin etkilerinin in silico gösterilmesi. *Kırşehir Ahi Evran Üniversitesi Ziraat Fakültesi Dergisi, 3*(2), 190–199.

Upadhyay, P., & Tewari, A. K. (2019). Evaluation of botanical extracts, animal wastes, organic and inorganic salts, micronutrients and bio-agents against *Sclerotinia sclerotiorum* (Lib.) de Bary: A cause of sclerotinia rot of rapeseed-mustard under field conditions. *Bulletin of Environment, Pharmacology and Life Sciences, 8*(12), 60–65.

Uygun, N., Ulusoy, M. R., & Satar, S. (2016). Biyolojik mücadele. *Türkiye Biyolojik Mücadele Dergisi, 1*(1), 1–14.

Van Lenteren, J. C. (2000). A greenhouse without pesticides: Fact or fantasy? *Crop Protection, 19*(6), 375–384.

Wallock-Richards, D., Doherty, C. J., Doherty, L., Clarke, D. J., Place, M., Govan, J. R., & Campopiano, D. J. (2014). Garlic revisited: Antimicrobial activity of allicin-containing garlic extracts against *Burkholderia cepacia* complex. *PLOS ONE, 9*(12), e112726.